

Inelastic tunneling through mesoscopic structures

Kristjan Haule

Jožef Stefan Institute, Ljubljana, Slovenia

Janez Bonča

Jožef Stefan Institute, Ljubljana, Slovenia

and FMF, University of Ljubljana, Ljubljana, Slovenia

(Received 4 August 1998; revised manuscript received 8 December 1998)

Our objective is to study resonant tunneling of an electron in the presence of inelastic scattering by optical phonons. Using a recently developed technique, based on exact mapping of a many-body problem onto a one-body problem, we compute transmission through a single site at finite temperatures. We also compute current through a single site at finite temperatures and an arbitrary strength of the potential drop over the tunneling region. Transmission vs incident electron energy at finite temperatures displays additional peaks due to phonon absorption processes. Current at a voltage bias smaller than the phonon frequency is dominated by elastic processes. We apply the method to an electron tunneling through the Aharonov-Bohm ring coupled to optical phonons. The elastic part of electron-phonon scattering does not affect the phase of the electron. Dephasing occurs only through inelastic processes. [S0163-1829(99)11819-8]

I. INTRODUCTION

Advances in crystal-growth techniques and constantly shrinking semiconductor devices have motivated researchers to study electron tunneling in mesoscopic structures. The ability to grow nearly perfect microscopic devices has enabled experimental confirmation of many theoretical predictions based on rather simple microscopic models. In particular, some basic ideas about electron-phonon interaction motivated an explanation of the seemingly unusual properties of electrons tunneling in the presence of interactions with phonons and other excitations,^{1,2} where inelastic processes affect the peak-to-valley current ratio. This is important in device applications. Another line of research in mesoscopic structures is focused on Aharonov-Bohm oscillations in a mesoscopic ring.³⁻⁷ Special attention in this field is devoted to a loss of coherence, or dephasing, under the influence of inelastic scattering leading to suppression of hc/e oscillations.

Most previous treatments of this problem use a Green's-function approach often based on Keldysh formalism.⁸⁻¹² Exact solutions were obtained only in the wide-band limit and for certain special cases. Calculating the current in the presence of inelastic scattering, some authors work in the limit of large bias through the tunneling region. This results in neglecting the backward current and the exclusion of the filled final states.⁸ The independent-boson model has been successfully used to directly solve the one-dimensional Schrödinger equation for arbitrary barrier structure.¹³ The transfer-matrix approach has proven very efficient to model realistic barrier structures and compare calculations to experiment. Electron-phonon interaction is in this case treated via Fermi's golden rule.¹⁴ Other attempts rely on linear-response theory using the Kubo formula.⁷

This work is based on a recently developed method¹⁵ for studying inelastic electron tunneling. The method provides exact solutions for tunneling problems where a single elec-

tron tunnels in the presence of phonon degrees of freedom that are limited to the tunneling region. The main goals of this work are (a) to extend the existing method to finite temperatures, (b) to derive an approximate formula for electric current in the presence of inelastic degrees of freedom, and (c) to apply developed formalism to the case of a single site coupled to phonons as well as to an Aharonov-Bohm ring. The method we use allows numerically exact calculation of transmission at finite temperatures. We treat bands exactly in contrast to some previous works,^{8,9} where the wide-band limit was used. We derive an approximate formula for the electric current that contains an exact expression for the transmission matrix and provides results for the current at an arbitrary voltage drop through the tunneling region, as precisely as the one-electron approximation allows. In deriving the equation for current we treat the forward and backward current on an equal footing. We also take into account exclusion from the filled final states. However, we neglect the effects of Coulomb interaction and phonon mediated electron-electron interaction. Our method can be applied to complicated tunneling structures containing multiple-phonon degrees of freedom. In this work we present results for two cases: (i) a single site coupled to optical phonons and (ii) to an Aharonov-Bohm ring in a tight-binding approximation where each site is coupled to Einstein phonons. We study the effect of inelastic scattering on transmission and consequently the current through the ring. We finally comment on the effect of inelastic scattering on Aharonov-Bohm oscillations.

This work is organized as follows. In Sec. II we introduce the Hamiltonian for resonant tunneling in the presence of inelastic degrees of freedom (optical polarons) that are limited to a small region of space. We describe the method and derive an approximate equation for current. In Sec. III we present results for transmission and current, at zero and finite temperature, through a single site coupled to phonons. In Sec. IV we give results for transmission and current at zero

temperature through the Aharonov-Bohm ring. Concluding remarks and suggestions for future work are presented in Sec. V.

II. METHOD

The Hamiltonian we use can be written as a sum of the electron part H_{el} , the phonon part H_{ph} , and finally the electron-phonon interaction H_{el-ph}

$$H = H_{el} + H_{ph} + H_{el-ph},$$

$$H_{el} = \sum_j \epsilon_j c_j^\dagger c_j - \sum_{j,k} t_{j,k} (c_j^\dagger c_k + \text{H.c.}), \quad (1)$$

$$H_{ph} = \omega \sum_m a_m^\dagger a_m,$$

$$H_{el-ph} = - \sum_j \lambda_j c_j^\dagger c_j (a_j^\dagger + a_j).$$

The potential, ϵ_j on site j , can describe a tunnel barrier or a voltage bias. Since we treat left and right lead exactly, we choose a constant potential $\epsilon_{L(R)}$ within the left (right) lead. The voltage drop is thus limited to the tunneling region. The hopping amplitude $t_{j,k}$ is set to t within the leads, t_0 is the hopping amplitude from the lead to the tunneling region, and λ_j is the (diagonal) coupling of an electron on site j to the phonon mode on the same site. Electron-phonon coupling is limited to the tunneling region. We consider dispersionless Einstein phonons with frequency ω .

The problem we are facing is to solve a scattering problem of a single electron in the presence of inelastic degrees of freedom. Since a detailed explanation of the method was given in previous work,¹⁵ we will present only a short overview that is necessary for the reader to understand our generalization to finite temperature and computation of the current.

Consider for simplicity the case where the tunneling region consists of a single site ($j=0$) with a single phonon mode that couples to the electron density on site 0 (see the lowest row in Fig. 1). Hopping matrix elements are $t_{k,l} = t$ for the lead nearest neighbors $k, l \neq 0$, and $t_{k,l} = t_0$ between site 0 and sites ± 1 . The wave function can be written as $\psi_{(j,n)}$, where the site index j represents the position of the electron and n represents the number of phonons on the site $j=0$. The Schrödinger equation can be written for this simple problem in the compact form,

$$E \psi_{(j,n)} = \epsilon_j \psi_{(j,n)} - \sum_{\langle j,k \rangle} t_{jk} \psi_{(k,n)} + \omega n \psi_{(j,n)} - \lambda \delta_{j,0} (\sqrt{n+1} \psi_{(j,n+1)} + \sqrt{n} \psi_{(j,n-1)}). \quad (2)$$

It is already apparent from Eq. (2) that a one-dimensional many-body problem, consisting of an electron and different numbers of phonon quanta, can be visualized as an effective two-dimensional one-body problem with n as the second dimension. For a better perception we present Eq. (2) graphically in Fig. 1 as a tight-binding model in two dimensions. For illustrative purposes we have restricted the variational space to a maximum $N_{ph} = 2$ phonon quanta. At zero tem-

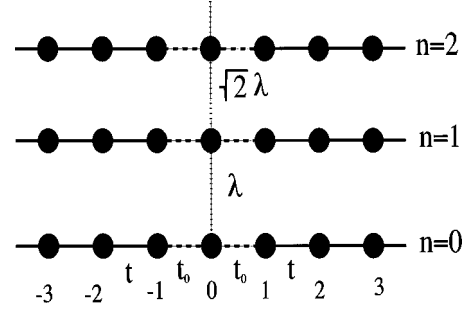


FIG. 1. Each dot represents a basis-state wave function $\psi_{(j,n)}$ in the many-body Hilbert space. The lowest row of dots are the sites $j = -3, \dots, 3$ with diagonal energies ϵ_j . The rows above represent the same sites with $n = 1, 2$ phonon quanta on the site $j = 0$. Their diagonal energies are $\epsilon_j + \omega$ and $\epsilon_j + 2\omega$, respectively. The bonds represent nonzero off-diagonal matrix elements in the Hamiltonian. The horizontal bonds are the hopping amplitudes $t_{j,k}$. The vertical bonds represent the electron-phonon interaction. The dots can also be interpreted as Wannier orbitals in an equivalent one-body tight-binding model.

perature, an electron incident from the left is an incoming plane wave on the lower left lead (there are no excited phonons on site 0). It has an amplitude to exit on any of the six leads, corresponding to elastic and inelastic backscattering and transmission. At finite temperatures a finite number of phonon quanta n are excited on site $j = 0$ before scattering with the probability $P(n) = (1 - e^{-\beta\omega}) e^{-n\beta\omega}$. Thus an electron can enter on any of the horizontal leads corresponding to different n . We can solve the set of equations in Eq. (2) taking into account the boundary condition specifying that an electron can enter only through one lead at a time. Solutions within the leads for an electron approaching from the left are

$$\begin{aligned} \psi_{(j < 0, n)} &= A^{(n)} \exp(ik_L^{(n)} j) + B^{(n)} \exp(-ik_L^{(n)} j), \\ \psi_{(j > 0, m)} &= C^{(m)} \exp(ik_R^{(m)} j), \\ \psi_{(j < 0, m \neq n)} &= B^{(m)} \exp(-ik_L^{(m)} j), \end{aligned} \quad (3)$$

where $n(m)$ represents the number of excited phonon quanta before (after) scattering, $A^{(n)}$ is the amplitude of the incident wave, and $B^{(m)}$ and $C^{(m)}$ represent reflection and transmission amplitudes. Wave vectors are defined by the conservation of total energy,

$$\epsilon_L + n\omega - 2t \cos(k_L^{(n)}) = \epsilon_{L(R)} + m\omega - 2t \cos(k_L^{(m)}). \quad (4)$$

Using the pruning technique¹⁵ we can remove all the leads that contain outgoing waves from the calculation. We are thus left with a system of linear equations that connect wave functions on the central site $\psi_{(0,n)}$ with the lead that carries the incoming electron. This problem can be solved easily by recursion for essentially any number of phonon quanta. The transmission matrix $T_{L \rightarrow R}^{n,m}(\epsilon, \epsilon')$ is defined as¹⁵

$$T_{L \rightarrow R}^{n,m}(\epsilon, \epsilon') = \left| \frac{C^{(m)}}{A^{(n)}} \right|^2 \frac{\sin k_R^{(m)}}{\sin k_L^{(n)}}, \quad (5)$$

where $n(m)$ represent incoming (outgoing) channels [by a channel we denote the lead with a specified number of phonons (n)], and ϵ (ϵ') are incoming (outgoing) electron

energies counted from the middle of the band, i.e., $\epsilon = -2t \cos(k_L^{(n)})$. We define the total and elastic transmission as a sum over all incoming channels n , weighted by the probability $P(n)$ and a sum over all outgoing channels. Since $P(n)$ depends on the temperature of the tunneling region, we must assume that the temperature of the tunneling region is well defined. This is achieved by coupling it to the external heat bath:

$$T_{tot}(\epsilon) = \sum_{n,m} P(n) T_{L \rightarrow R}^{(n,m)}(\epsilon, \epsilon'), \quad (6)$$

$$T_{elast}(\epsilon) = \sum_n P(n) T_{L \rightarrow R}^{(n,n)}(\epsilon, \epsilon'). \quad (7)$$

Using the presented technique we can compute transmission at zero and finite temperatures with any desired accuracy. However, transmission is not in principle a directly measurable quantity. One has to compute electric current in order to provide a measurable quantity. The total transmission as defined in Eq. (6) enters the equation for current only in the case of a high-voltage bias where neither the backward current nor the exclusion of filled states in the right lead are taken into account.⁸

In deriving the equation for the current we start by observing that inelastic processes can be viewed as multichannel electron tunneling. The current from the left lead, due to an electron entering the tunneling region through a channel n and exiting through m , is given by the integral over the incoming momenta $\hbar dk_L^{(n)}$ times the velocity of the incoming electron $v_L = (1/\hbar) d\epsilon/dk_L^{(n)}$, times the transmission probability $T_{L \rightarrow R}^{(n,m)}(\epsilon, \epsilon')$, times the appropriate combination of Fermi functions from the left and the right lead. The total current from the left is expressed as a sum over all channels weighted with the appropriate Boltzmann factor. The net current is given finally by the difference between the right- and the left-flowing currents

$$J = \frac{e}{\pi\hbar} \int_{-2t}^{2t} d\epsilon \sum_{n,m} P(n) T_{L \rightarrow R}^{(n,m)}(\epsilon, \epsilon') f_L(\epsilon) (1 - f_R(\epsilon')) - \frac{e}{\pi\hbar} \int_{-2t}^{2t} d\epsilon' \sum_{m,n} P(m) T_{R \rightarrow L}^{(m,n)}(\epsilon', \epsilon) f_R(\epsilon') (1 - f_L(\epsilon)), \quad (8)$$

where $T_{R \rightarrow L}^{(m,n)}$ is the transmission matrix for an electron coming from the right. Electron energies are constrained by the energy conservation law, $\epsilon + \epsilon_L + n\omega = \epsilon' + \epsilon_R + m\omega$. Fermi functions $f_{L(R)}$ describe the left (right) lead. We can write equation for current (8) in a more compact form, by taking advantage of the time-reversal symmetry under which $T_{R \rightarrow L}^{(m,n)}(\epsilon', \epsilon) \rightarrow T_{L \rightarrow R}^{(n,m)}(\epsilon, \epsilon')$ and the fact that the transmission matrix is nonzero when both electron energies ϵ and ϵ' are within the band,

$$J_{tot} = \frac{e}{\pi\hbar} \int_{-2t}^{2t} d\epsilon \sum_{n,m} T_{L \rightarrow R}^{(n,m)}(\epsilon, \epsilon') [P(n) f_L(\epsilon) (1 - f_R(\epsilon')) - P(m) f_R(\epsilon') (1 - f_L(\epsilon))]. \quad (9)$$

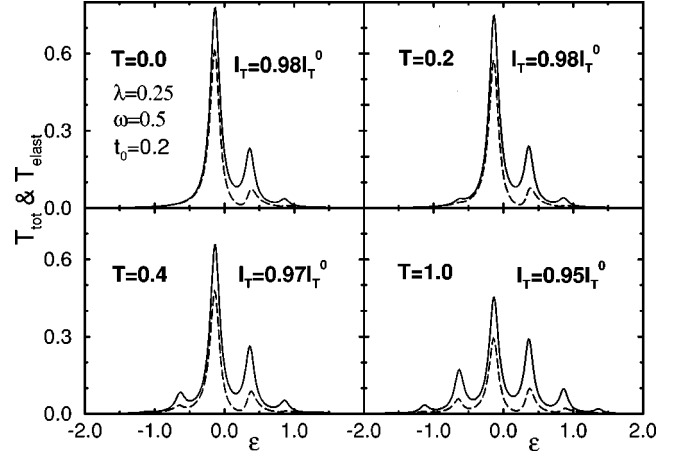


FIG. 2. Transmission probability as a function of the incident electron energy calculated for different temperatures T . The heavy line is the total transmission T_{tot} , and the dashed (lower) line the elastic part T_{elast} . The parameters of the Hamiltonian are $\lambda = 0.25$, $\epsilon_l = \epsilon_r = \epsilon_0 = 0.0$ (no voltage drop across the dot), $t_0 = 0.2$, $\omega = 0.5$, and $N_{ph} = 17$. Also presented are sum rules where $I_T^0 = 2\pi t(t_0/t)^2$.

We can also compute the elastic contribution to the total current in Eq. (9) by imposing the constraint of elastic tunneling $n = m$:

$$J_{elast} = \frac{e}{\pi\hbar} \int_{-2t}^{2t} d\epsilon \sum_n T_{L \rightarrow R}^{(n,n)}(\epsilon, \epsilon + \Delta\mu) P(n) \times [f_L(\epsilon) - f_R(\epsilon + \Delta\mu)], \quad (10)$$

where $\Delta\mu = \epsilon_L - \epsilon_R$. The total energy of the electron $E = \epsilon + \epsilon_L = \epsilon' + \epsilon_R$ is in this case conserved. In the limit of zero temperature Eq. (10) gives the correct result for elastic tunneling (see, e.g., Ref. 8).

Our derivation of Eq. (9) is based on the one-electron approximation which leads to neglecting many-body effects as are (a) the Coulomb repulsion and (b) phonon mediated electron-electron interaction. Closely connected to the latter is our assumption that phonon distribution $P(n)$ is independent of electron current through the tunneling region. The validity of Eq. (9) is therefore limited to cases when the current is small and the tunneling region is strongly coupled to the external heat bath. This can be achieved even at large voltage bias when coupling to the leads is weak, i.e., $t_0 \ll t$.

III. RESULTS FOR A SINGLE SITE

In our calculation we have set the hopping within the lead to $t = 1$. The maximum number of allowed phonon quanta N_{ph} was selected such that results fully converged for all chosen parameters of the system at different temperatures.

A. Transmission

In Fig. 2 we show the total and elastic transmission [Eqs. (6) and (7)] as a function of the incoming electron energy ϵ at different temperatures. At low temperatures we see a central peak positioned at $\epsilon \sim \epsilon_0 - \lambda^2/\omega$, a one phonon side peak at $\epsilon \sim \epsilon_0 + \omega - \lambda^2/\omega$, and a small two phonon peak at higher ϵ . Positions of the peaks approximately correspond to po-

laron energies, given by $\epsilon_{pol}(n) = \epsilon_0 - \lambda^2/\omega + n\omega$, where n represents the n th excited state of a polaron. By polaron we symbolize a state of an electron, coupled to phonon degrees of freedom located on the same site in the limit when $t_0 \rightarrow 0$. It is important to emphasize that all peaks have an elastic and an inelastic contribution (see also Refs. 8 and 15). Elastic contributions correspond to tunneling through the ground or the excited state of a polaron without emitting (or absorbing) a phonon. Inelastic parts correspond to tunneling through a given state with simultaneous phonon emission or absorption. At zero temperature only phonon emission processes are allowed since before tunneling the phonon state contains no phonons.

At finite temperature other processes can take place. As an electron enters the tunneling region there may be one or more phonons excited in the system. The side peak at $\epsilon \sim \epsilon_0 - \omega - \lambda^2/\omega$ is due to a process when an electron enters the tunneling region and absorbs a phonon. Such a process has been observed by Cai *et al.*¹³ As the temperature increases more inelastic channels open for electron tunneling, giving rise to an increased strength of side peaks. Interestingly enough, the sum rule, valid at zero temperature and within the wide-band approximation^{8,9} $I_T^0 = \int d\epsilon T_{tot}(\epsilon) = 2\pi t(t_0/t)^2$, remains valid in our numerically exact approach at small temperatures, and it changes at most 5% at large temperatures (see values in the inset). We would like to stress that sum rules I_T^0 (and I_J^0 , see the next subsection), defined in the work of Wingreen *et al.*,⁸ do not represent sum rules in a strict sense. They instead represent identities that are derived on the basis of two main approximations: dispersionless bands and a large bias limit used when calculating the current. Even though our calculations are not limited by these approximations, we nevertheless chose to compare integrals of transmission with I_T^0 and in the next chapter integrals of current with I_J^0 . As the temperature rises, peaks due to multiphonon processes increase in strength. It almost seems as though finite temperature increases the effective coupling strength λ as seen in Ref. 12. However, an increased coupling strength would also shift the peaks. Peaks in Fig. 2 do not shift with increasing temperature. The increased strength of multiphonon side peaks is a consequence of the increased number of excited phonons in the tunneling region at higher temperatures.

B. Current through a single site

We continue with a discussion of current. The relative positioning of bands and the choice of chemical potentials in the calculation are presented schematically in Fig. 3. We have positioned the chemical potentials in the left and right lead in the middle of each band. This situation corresponds to both leads being made from the same metal. The value of the chemical potential within each lead is constant and corresponds to asymptotic values in the leads. Bands are shifted symmetrically due to an applied bias $\Delta\mu$ i.e., $\epsilon_L = \Delta\mu/2$ and $\epsilon_R = -\Delta\mu/2$, thus $\epsilon_L - \epsilon_R = \Delta\mu = eV$; where V represents the potential drop across the tunneling region.

In Fig. 4 we present the total and elastic current vs ϵ_0 (the on-site energy of the site $j=0$) for four different values of $\Delta\mu$. At a small $\Delta\mu = 0.02 \ll \omega$ there is no inelastic contribution to the current (solid and dashed curves overlap). The

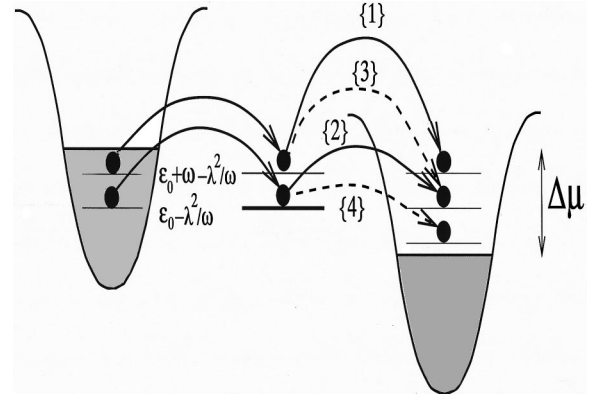


FIG. 3. A schematic representation of the positioning of the bands. Some elastic and inelastic processes that contribute to the total current are shown. Shaded areas represent filled one-electron states. In elastic processes ({1} and {2}) the total electron energy is conserved $\epsilon + \epsilon_L = \epsilon' + \epsilon_R$, while in inelastic ones ({3} and {4}) it is not. For clarity, only zero- and one-phonon states on the central site are included.

main reason for this interesting effect is that the chemical potential difference across the tunneling region is smaller than the minimum energy change ω necessary for the inelastic tunneling. The necessary condition for an electron, with an incoming energy ϵ , to contribute to the current at $T=0$, besides having a finite tunneling rate, can be expressed with two inequalities: $\epsilon + \epsilon_L < \mu_L$, and $\epsilon' + \epsilon_R + m\omega > \mu_R$. At small $\Delta\mu$ this condition leads to well defined peaks in the $J_{tot,elast}(\epsilon_0)$ curves since only electrons with a total energy in a narrow interval between the left and right chemical potential can give rise to current. Therefore only processes labeled by {1} and {2} in Fig. 3 contribute to formation of the

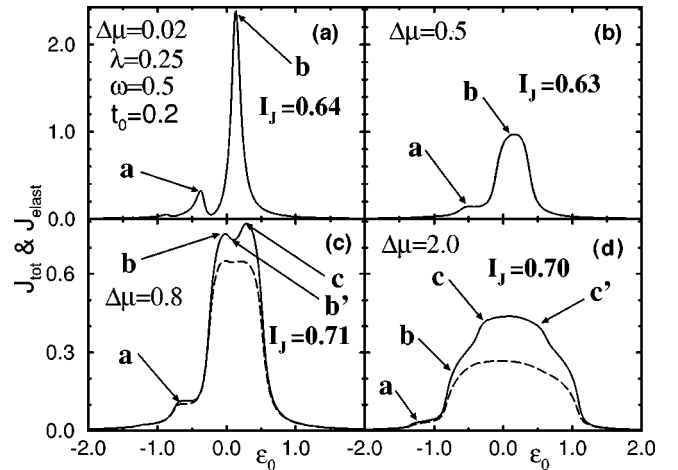


FIG. 4. The total current J_{tot} (solid line) and elastic current J_{elast} (dashed line) vs ϵ_0 at $T=0$ for four different choices of $\Delta\mu$. All curves are in units of I_J^0 (see definition below). Note also that the ordinates in figures (a) and (b) are different than in (c) and (d). Current flows at different ϵ_0 through different channels. Opening or closing of different channels (processes) as ϵ_0 increases is reflected in peaks, shoulders, or dips in the curves. Those anomalies (labeled by small letters) at different $\Delta\mu$ correspond to the following processes (see Fig. 3) (a) $a:\{1\}$, $b:\{2\}$; (b) $a:\{1\}$, $b:\{2\}$; (c) $a:\{1\}$, $b:\{1,2,3\}$, $b':\{2\}$, $c:\{2,4\}$; (d) $a:\{1\}$, $b:\{1,2,3\}$, $c:\{1,2,3,4\}$, $c':\{2,4\}$.

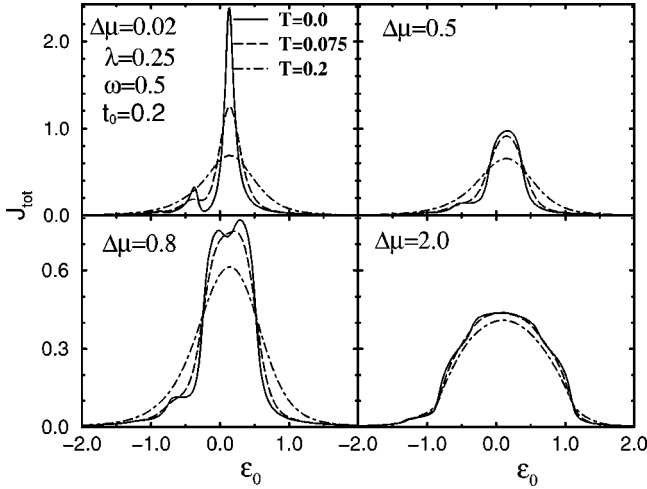


FIG. 5. The total current J_{tot} vs ϵ_0 at $T=0, 0.075,$ and 0.2 for four different choices of $\Delta\mu$. All curves are in units of I_J^0 . All other parameters are the same as in Fig. 4.

side (a) and the central peak (b), respectively. We should stress that phonons nevertheless still play an important role even at small voltage biases. The side peak (a) at approximately $\epsilon_0 = \lambda^2/\omega - \omega$ represents an elastic process where an electron elastically tunnels through the first excited state of a polaron whose energy is $\epsilon_{pol}(1) = -\lambda^2/\omega + \omega$, while the main peak (b) corresponds to elastic tunneling through the polaron ground state $\epsilon_{pol}(0)$.

As $\Delta\mu$ increases to $\Delta\mu = \omega = 0.5$ the side peak develops into a shoulder and moves towards lower $\epsilon_0 \sim \omega^2/\lambda - \omega - \Delta\mu/2$ while the central peak broadens. This is a consequence of separating the left and right chemical potentials and thus imposing less restrictive conditions on the tunneling electron energies. In particular, the broadening of the central peak is caused by simultaneous tunneling through processes labeled {1} and {2} in Fig. 3; also note the figure caption. Inelastic contribution is still small.

The main features appearing at larger bias, i.e., $\Delta\mu = 0.8$, are (a) the emergence of the inelastic current (the solid and dashed lines do not overlap) and (b) development of a new structure in the central peak region. The appearance of the inelastic current is caused by the opening of the inelastic channels at $\Delta\mu > \omega$. The new structure in the central peak region is caused by opening and closing of elastic or inelastic tunneling channels as ϵ_0 increases (see caption to Fig. 4). At even larger bias $\Delta\mu = 4\omega = 2.0$ the current $J_{tot}(\epsilon_0)$ broadens even though the effects of different channel contributions are still visible. The inelastic current increases relatively to the elastic current.

We have also computed integrals $I_J = \int d\epsilon_0 J(\epsilon_0)$ that according to Wingreen *et al.*⁸ should equal $I_J^0 = (e/\pi\hbar)2\pi t(t_0/t)^2\Delta\mu$. Our findings are that even though the current does scale with $\Delta\mu$, nevertheless, our integrals deviate from sum rules that exist in the wide band and large bias limit. The main reason is that the current flows through only selected channels allowed by the difference in the chemical potentials and not through all the channels as is the case in the limit of large bias and wide bands.

The effect of finite temperatures on the total current is presented in Fig. 5. In contrast to the case of the total trans-

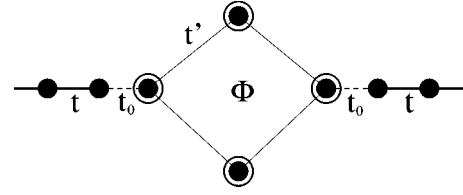


FIG. 6. Schematic representation of the Hamiltonian describing the Aharonov-Bohm ring. Dots surrounded by circles represents sites coupled to Einstein phonons. For simplicity we have chosen on-site energies on the ring to be constant $\epsilon_j = \epsilon_0$. Magnetic flux Φ penetrates the center of the ring.

mission we were unable to obtain additional peaks corresponding to phonon absorption processes. With increasing temperature the smearing by the Fermi functions overcomes development of those peaks. The effects of raising the temperature are more intense at smaller biases where peaks are narrower. Phonon side peaks disappear around $T \sim \omega/2$.

IV. TUNNELING THROUGH AHARONOV-BOHM RING

Next, we consider tunneling and consequently the current through an Aharonov-Bohm ring. The purpose of this section is to investigate the effect of dephasing by phonon modes on an electron as it tunnels through a ring. In detail, we will focus on the effect of dephasing on the transmission and current through the ring.

The model is schematically presented in Fig. 6. The ring consists of four sites, connected by hopping matrix element t' , that are coupled to two connecting leads with the hopping matrix element t_0 . Each site of the ring is coupled to an Einstein phonon mode with frequency ω . There are four different phonon modes (one on each site) with identical frequency ω . A magnetic flux is penetrating the circle. This is reflected in an additional phase $\pm\phi$ that the electron gains each time it hops from one site on the circle to another. The electron part of the Hamiltonian (1), describing hopping within the ring, has to be modified in order to encompass the effect of a vector potential

$$H_{el} = \epsilon_0 \sum_j c_j^\dagger c_j - t' \sum_j (e^{i\phi} c_j^\dagger c_{j+1} + \text{H.c.}), \quad (11)$$

where the sum runs over the sites of the ring. All on-site energies within the ring were, for simplicity, set to ϵ_0 . We solve this problem using the method described above (see also Ref. 15), and generalized to many phonon degrees of freedom. By increasing the maximum allowed number of phonons N_{ph} on each site this problem can be solved with any desired accuracy. There are of course computer limitations. In practice, for moderate electron-phonon coupling and low temperatures, $N_{ph} = 3$ is enough to obtain results with at least 1% accuracy. The number of many-body states increases as $N_{st} = N(N_{ph} + 1)^N = 1024$, which corresponds to the number of channels $N_{ch} = 2N_{st}$. N is the number of sites in the ring. In a scattering problem where the energy of the incoming electron is known in advance, we have to solve a large $(N_{st} \times N_{st})$ sparse system of complex linear equations for each ϵ . Due to computer limitations, we restricted calculations to zero temperature.

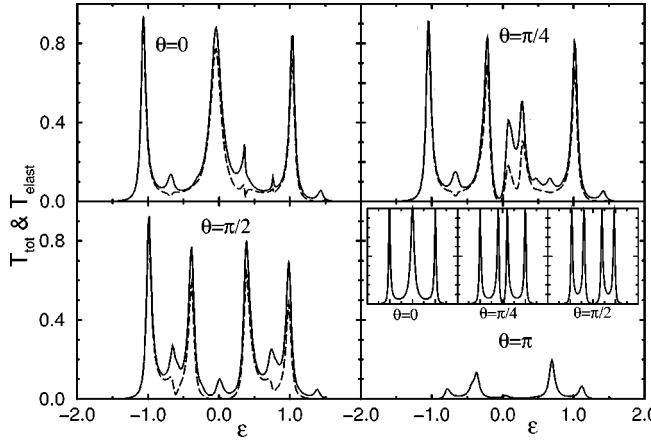


FIG. 7. Transmission probability as a function of the incident electron energy ϵ at $T=0$ calculated at different θ . The heavy line is the total transmission T_{tot} , and the dashed (lower) line the elastic part T_{elast} . The parameters of the Hamiltonian are $\lambda=0.2$, $\epsilon_l = \epsilon_r = \epsilon_0 = 0.0$, $t_0 = 0.3$, $\omega_0 = 0.4$, $t' = 0.5$ and $N_{ph} = 3$. In the inset we show (insets are in the same units as the rest of the figures in Fig. 7) transmission T_{elast} for the noninteracting case, i.e., $\lambda = 0$.

We have computed the total and elastic transmission vs ϵ through an Aharonov-Bohm ring at different values of total phase, $\theta = \phi N$. In Fig. 7 we show results for the total and elastic transmission through a ring. Positions of the main peaks are approximately located close to energies corresponding to solutions of a tight-binding problem on a $N=4$ site ring with a phase ϕ , i.e., $E(k) = -2t' \cos(k + \phi)$ for $k = 2\pi i/N$. One and two phonon side peaks (shoulders) are also visible at approximately $\epsilon_{n,k} = E(k) + n\omega$. The height and the width of the main peaks change substantially when the position of the main peak coincides with the position of the phonon-side peak (see $\theta = \pi/4$).

The most interesting result is found at $\theta = \pi$ which corresponds to a phase, where in the case of noninteracting tun-

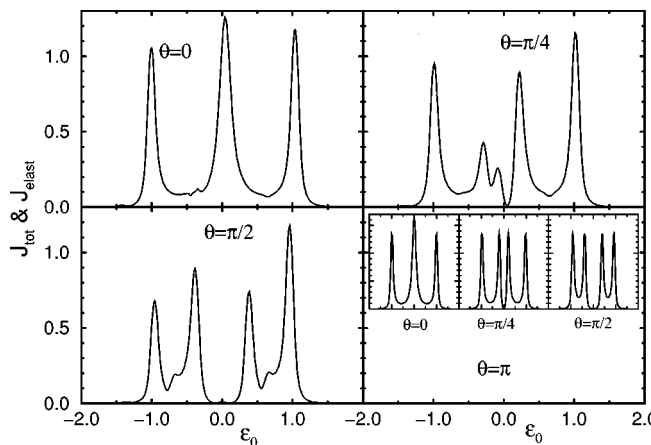


FIG. 8. The total current J_{tot} (solid line) and elastic current J_{elast} (dashed line) calculated at $\Delta\mu=0.1$ vs ϵ_0 at $T=0$ for four different choices of phase θ . All curves are in units of I_j^0 . Note that the solid and the dashed lines overlap indicating $J_{tot} = J_{elast}$. As in the previous section we set $\epsilon_L = \Delta\mu/2$ and $\epsilon_R = -\Delta\mu/2$. The rest of the parameters remain the same as in Fig. 7. In the inset we show for comparison the elastic current J_{elast} for the noninteracting case. Insets are in the same units as the rest of the Fig. 8.

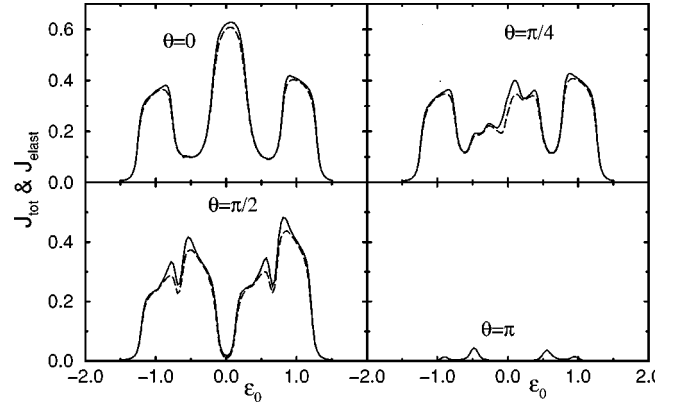


FIG. 9. The total current J_{tot} (solid line) and elastic current J_{elast} (dashed line) calculated at $\Delta\mu=0.5$ vs ϵ_0 at $T=0$ for four different choices of phase θ . The rest is the same as in Fig. 8.

neling due to negative interference, transmission is exactly zero for any ϵ . At finite electron-phonon coupling we obtain, for $\theta = \pi$, a finite total transmission. However, the elastic part of transmission remains exactly (down to numerical accuracy) zero. This result is surprising considering that elastic tunneling processes are possible when an electron first emits and then reabsorbs a phonon. A phase shift that the electron undergoes while emitting a phonon is thus exactly canceled by the phase shift after reabsorbing a phonon. Tunneling at $\theta = \pi$ is therefore exclusively due to inelastic processes. This finding is in accordance with the well accepted fact that impurity (elastic) scattering cannot destroy Aharonov-Bohm oscillations,¹⁶ since it does not cause phase decoherence.

Furthermore, we have calculated current, Eqs. (9) and (10), vs ϵ_0 through the Aharonov-Bohm ring at small bias, $\Delta\mu=0.1$, zero temperature and different θ . These results are presented in Fig. 8. As we have already shown in the previous section, only elastic current can flow at small bias. Nevertheless, effects of electron-phonon interaction are clearly visible. There is no net current at $\theta = \pi$ since only the elastic part of the transmission can contribute to the elastic current. We predict that at small bias $\Delta\mu \ll \omega$ Aharonov-Bohm oscillations through the mesoscopic Aharonov-Bohm ring should not diminish significantly due to electron-phonon coupling, where coupling is limited to optical phonons.

Last, we present results for current through the Aharonov-Bohm ring at large bias, $\Delta\mu = 0.5 > \omega$. Results are presented in Fig. 9. Two most important effects of larger bias are broadening of the peaks and the appearance of the inelastic current ($J_{tot} - J_{elast}$). As a consequence of dephasing by inelastic scattering we observe finite inelastic current at $\theta = \pi$.

V. CONCLUSIONS

In summary, we have extended a numerically exact method,¹⁵ for inelastic tunneling, to calculate transmission through a single site coupled to phonons at finite temperatures. We have further proposed an approximate formula for current based on exact results for the transmission matrix, taking into account filled Fermi seas left and right from the tunneling region and left- and right-flowing currents. The presented formalism gives correct result in the limit of elastic current. Our approach is entirely based on a one-electron

approximation. By investigating tunneling through an Aharonov-Bohm ring coupled to optic phonons, we have obtained numerically exact results for transmission at zero temperature. We have also computed the current through the ring.

We highlight some of the important findings of this work as follows.

Transmission through a single site vs incident electron energy at finite temperatures displays additional peaks due to phonon absorption processes. The sum rule I_T , valid in the wide-band limit and zero temperatures, remains approximately obeyed in our exact approach even at finite temperatures. Deviations are within 5% even at temperatures $T > \omega$.

Current through a single site mimics the transmission curve at small bias $\Delta\mu \ll \omega$ and $T=0$. At voltage bias $\Delta\mu < \omega$, and zero temperature only current due to elastic processes is possible, since inelastic processes are excluded due to filled final states. With increasing temperature, features due to inelastic processes disappear around $T \sim \omega/2$. Phonon absorption peaks do not appear in the current at finite temperatures since they are smeared by Fermi functions.

Transmission through the Aharonov-Bohm ring consists only of inelastic transmission at $\theta = \pi$. The lack of elastic transmission is considered as evidence that elastic processes, even though they are a part of inelastic electron-phonon scattering, do not change the phase of the tunneling electron. We have thus presented numerical proof that elastic scattering by

phonons does not affect Aharonov-Bohm oscillations. Dephasing occurs only through inelastic processes. This is the reason why interference effects, measured at small bias $\Delta\mu < \omega$ across the tunneling region, display strong Aharonov-Bohm oscillations by changing the flux through the ring. Calculation of current at larger bias $\Delta\mu > \omega$ shows that only inelastic current flows through the Aharonov-Bohm ring in the case when $\theta = \pi$. The voltage drop over the region has to be larger than the minimal energy difference necessary for inelastic scattering i.e., $\Delta\mu > \omega$.

It would be interesting to study the tunneling through the Aharonov-Bohm ring at finite temperatures. Such computation would demand larger Hilbert space and more computational time. Our method also allows the implementation of the nonlinear electron-phonon interaction and linear and nonlinear phonon-phonon interactions. It would be fascinating to investigate how phonon-phonon interactions, leading to internal phonon dynamics, affect dephasing of the tunneling electrons through an Aharonov-Bohm ring.

ACKNOWLEDGMENTS

One of the authors (J.B.) gratefully acknowledges support by the SLO USA grant and the hospitality of Los Alamos National Laboratory. We thank Anton Ramšak, Peter Prelovšek, and Stuart Trugman for stimulating discussions, and Mike Stout for his careful reading of the manuscript.

¹V. J. Goldman, D. C. Tsui, and J. E. Cunningham, Phys. Rev. B **36**, 7635 (1987).

²L. P. Kouwenhoven, S. Jauhar, J. Orenstein, and P. L. McEuen, Phys. Rev. Lett. **73**, 3443 (1994).

³A. Yacoby, M. Heiblum, D. Mahalu, and H. Shtrikman, Phys. Rev. Lett. **74**, 4047 (1995).

⁴E. Buks, R. Schuster, M. Heiblum, D. Mahalu, V. Umansky, and H. Shtrikman, Phys. Rev. Lett. **77**, 4664 (1996).

⁵A. Stern, Y. Aharonov, and Y. Imry, Phys. Rev. A **41**, 3436 (1990).

⁶A. L. Yeyati and B. Büttiker, Phys. Rev. B **52**, R14 360 (1995).

⁷Shechao Feng, Phys. Lett. A **143**, 400 (1990).

⁸N. S. Wingreen, K. W. Jacobsen, and J. W. Wilkins, Phys. Rev. Lett. **61**, 1396 (1988); Phys. Rev. B **40**, 11 834 (1989).

⁹L. I. Glazman and R. I. Shekhter, Zh. Éksp. Teor. Fiz. **94**, 292

(1988) [Sov. Phys. JETP **67**, 163 (1988)].

¹⁰B. Y. Gelfand, S. Schmitt-Rink, and A. F. J. Levi, Phys. Rev. Lett. **62**, 1683 (1989).

¹¹J. A. Stóveng, H. Hauge, P. Lipavský, and V. Špička, Phys. Rev. B **44**, 13 595 (1991).

¹²M. Jonson, Phys. Rev. B **39**, 5924 (1989).

¹³W. Cai, T. F. Zheng, P. Hu, B. Yudanin, and M. Lax, Phys. Rev. Lett. **63**, 418 (1989); W. Cai, T. F. Zheng, P. Hu, and M. Lax, Mod. Phys. Lett. B **5**, 173 (1991).

¹⁴P. J. Turley and S. W. Teitsworth, Phys. Rev. B **44**, 3199 (1991); **44**, 8181 (1991); P. J. Turley, C. R. Wallis, S. W. Teitsworth, W. Li, and P. K. Bhattacharya, *ibid.* **47**, 12 640 (1993).

¹⁵J. Bonča and S. A. Trugman, Phys. Rev. Lett. **75**, 2566 (1995).

¹⁶S. Washburn and R. A. Webb, Adv. Phys. **35**, 375 (1986).